



ACCESS
Arctic Climate Change
Economy and Society



Project no. 265863

ACCESS
Arctic Climate Change, Economy and Society

Instrument: Collaborative Project
Thematic Priority: Ocean.2010-1 "Quantification of climate change impacts on economic sectors in the Arctic"

D4.45 – Recommendations on future Arctic observing systems

Due date of deliverable: **31/01/2015**

Actual submission date: **30/01/2015**

Start date of project: **March 1st, 2011**

Organisation name of lead contractor for this deliverable: **FastOpt**

Duration: **48 months**

Project co-funded by the European Commission within the Seventh Framework Programme (2007-2013)		
Dissemination Level		
PU	Public	
PP	Restricted to other programme participants (including the Commission Services)	
RE	Restricted to a group specified by the consortium (including the Commission Services)	
CO	Confidential, only for members of the consortium (including the Commission Services)	X



Contents

Table of Contents

1) Executive Summary.....	3
2) Detailed Study.....	4



1) Executive Summary

The Arctic climate system is undergoing a rapid transition. Such changes, in particular reductions in sea-ice extent, are impacting coastal communities and ecosystems and are enhancing the potential for resource extraction and shipping. In this context, the ability to anticipate anomalous ice conditions and in particular sea-ice hazards associated with seasonal-scale and short term variations in ice cover is essential. For example, in 2012, despite a long-term trend of greatly reduced ice cover in the Chukchi Sea off Alaska's coast, ice incursions and associated hazards led to early termination of the exploration season. In this context, high-quality predictions of the ice conditions are of paramount interest. Such predictions are typically performed by numerical models of the sea ice-ocean system. Within WP 1, FastOpt and OASys developed a framework for a modelling system to assist the design of the Arctic Observing System. The Arctic Observational Network Design (AOND) system was developed around the model of the coupled Arctic sea-ice ocean system NAOSIM. **The AOND system can evaluate candidate observational networks in terms of their constraint on target quantities of interest**, e.g. predicted ice area or volume for a given region. **Within WP 4** the system was **adapted to specific requirements for resource extraction** and used to evaluate hypothetical observational networks. For a demonstration, **we evaluated two idealised flight transects derived from NASA's Operation IceBridge airborne ice surveys** in terms of their potential to improve ten-day to five-month sea-ice forecasts. As target regions for the forecasts we selected the Chukchi Sea, an area particularly relevant for maritime traffic and offshore resource exploration as well as two areas related to the **Barnett Ice Severity Index (BSI)**, a standard measure of shipping conditions along the Alaskan coast that is routinely issued by ice services. Our analysis quantifies the benefits of sampling upstream of the target area and of reducing the sampling uncertainty. We **demonstrate** how observations of sea-ice and snow thickness can constrain the ice area in a target region and quantify the **complementarity of combining two flight transects**. We further quantify the benefit of improved atmospheric forecasts and a well-calibrated model. This is the **first time, such a quantitative analysis of the relative benefit of different sampling strategies is performed for the Arctic**. The evaluation of flight transects is only one application of the AOND system. Further potential applications are the evaluation of remote sensing concepts, potentially in combination with in situ measurements.

For our analysis we deliberately selected the year 2007, a year of particularly low ice extent, which one may regard as representative in terms of future ice conditions under climate change. Clearly, our quantitative results are specific to the conditions in this year. The present study has thus the character of a demonstration, and we **focus here on general lessons**. Our most general finding is that the **network performance depends on the question we ask**, i.e. on the target quantity. Next, **the longer the forecast time, the further upstream we have to sample**, rather than sampling over the target area. Further, we demonstrated in a quantitative way



how the **model dynamics transfer the observational information on one set of variables (snow and ice thickness) to another variable (ice area).**

When defining candidate networks to be evaluated it is **essential to take logistic constraints into account**. An example of a logistic constraint is the physical accessibility of an observational site, given the harsh environmental conditions in the Arctic. Another logistic constraint can be limited accessibility for political reasons. This could apply, for example, to the Siberian coastline. Logistic constraints can also be of technical nature, e.g. limited reach of an aircraft carrying the instrument. The AOND system is ignorant of such constraints, unless it is informed by the user through definition of logistically feasible candidate networks. At this point know how of observationalists is essential.

An essential input to the tool is the data uncertainty, which is the combination of uncertainties in the observational process and in modelling its counterpart (model uncertainty). Our models are based on fundamental equations that govern the processes controlling ice conditions. Uncertainty in model predictions arises from four sources: first, there is uncertainty in the atmospheric forcing data (such as wind velocity or temperature) driving the relevant processes. Second, there is uncertainty regarding the formulation of individual processes and their numerical implementation (structural uncertainty). Third, there are uncertain constants (process parameters) in the formulation of these processes (parametric uncertainty). Fourth, there is uncertainty about the state of the system at the beginning of the simulation (initial state). Typically the model uncertainty is assessed by modellers and the observational uncertainty by observationalists, i.e. the **AOND tool can be operated best by a team consisting of observationalists and modellers**.

We note that the above-mentioned model uncertainty to be provided to the tool does not necessarily need to refer to the model we use. As long as the response functions of our model are approximately correct, we can use the present system to simulate the observational impact on a assimilation system around a different model. For QND results to be valid beyond the model at hand, one has to used a well-validated model, which includes all relevant processes.

The current AOND system has the flexibility to also evaluate the potential of space missions or further in situ sampling strategies. There are a number of obvious ways to refine the present system. It can be extended to cover climate conditions of further years, possibly also representative of the state of the Arctic as expected under climate change. Also, one could add oceanic observations, further target quantities, or extend the control vector. Furthermore, rather than operating Arctic-wide, the same concept can be applied on smaller regional scale.

2) Detailed Study

Exploring the utility of quantitative network design in evaluating Arctic sea-ice thickness sampling strategies

T. Kaminski¹, F. Kauker², H. Eicken³, and M. Karcher²

¹FastOpt, Lerchenstraße 28a, 22767 Hamburg, Germany

²OASys, Lerchenstraße 28a, 22767 Hamburg, Germany

³Geophysical Institute, University of Alaska Fairbanks, P.O. Box 757320, Fairbanks, AK 99775-7320, U.S.A.

Correspondence to: T. Kaminski (thomas.kaminski@fastopt.com)

Abstract. We present a quantitative network design (QND) study of the Arctic sea ice-ocean system using a software tool that can evaluate hypothetical observational networks [in relation to external constraints] in a variational data assimilation system. For a demonstration, we evaluate two idealised flight transects derived from NASA's Operation IceBridge airborne ice surveys in terms of their potential to improve ten-day to five-month sea-ice forecasts. As target regions for the forecasts we select the Chukchi Sea, an area particularly relevant for maritime traffic and offshore resource exploration, as well as two areas related to the Barnett Ice Severity Index (BSI), a standard measure of shipping conditions along the Alaskan coast that is routinely issued by ice services. Our analysis quantifies the benefits of sampling upstream of the target area and of reducing the sampling uncertainty. We demonstrate how observations of sea-ice and snow thickness can constrain ice and snow variables in a target region and quantify the complementarity of combining two flight transects. We further quantify the benefit of improved atmospheric forecasts and a well-calibrated model.

1 Introduction

The Arctic climate system is undergoing a rapid transition. Such changes, in particular reductions in sea-ice extent, are impacting coastal communities and ecosystems and are enhancing the potential for resource extraction and shipping. In this context, the ability to anticipate anomalous ice conditions and in particular sea-ice hazards associated with seasonal-scale and short-term variations in ice cover is essential. For example, in 2012, despite a long-term trend of greatly reduced ice cover in the Chukchi Sea off Alaskas coast, ice incursions and associated hazards led to early termination of the exploration season (*Eicken and Mahoney, 2014*). In this context, high-quality predictions of the ice conditions are of paramount interest. Such predictions are typically performed by numerical models

of the sea ice-ocean system. These models are based on fundamental equations that govern the processes controlling ice conditions. Uncertainty in model predictions arises from four sources: first, there is uncertainty in the atmospheric forcing data (such as wind velocity or temperature) driving the relevant processes. Second, there is uncertainty regarding the formulation of individual processes and their numerical implementation (structural uncertainty). Third, there are uncertain constants (process parameters) in the formulation of these processes (parametric uncertainty). Fourth, there is uncertainty about the state of the system at the beginning of the simulation (initial state).

Observational information can be exploited to reduce these uncertainties. Currently there are several initiatives underway to extend and consolidate the observational network of the Arctic climate system, ranging, e.g., from the International Arctic Systems for Observing the Atmosphere and Surface (IASOAS) to the Global Terrestrial Network for Permafrost (GTN-P). Ideally, all observational data streams are interpreted simultaneously with the process information provided by the model to yield a consistent picture of the state of the Arctic system that balances all the observational constraints, taking into account the respective uncertainty ranges. Data assimilation systems that tie into prognostic models of the Arctic system are ideal tools for this integration task because they allow a variety of observations to be combined with the simulated dynamics of a model.

Quantitative Network Design (QND) is a technique that aims at designing an observational network with optimal performance. The approach is based on work by *Hardt and Scherbaum* (1994) who optimised the station locations for a seismographic network. It was first applied to the climate system by *Rayner et al.* (1996), who optimised the spatial distribution of atmospheric measurements of carbon dioxide. A series of QND studies (*Rayner and O'Brien*, 2001; *O'Brien and Rayner*, 2002; *Rayner et al.*, 2002) demonstrated the feasibility of the network design approach and delineated the requirements for the implementation of the first satellite mission designed to observe atmospheric CO₂ from space (*Crisp et al.*, 2004). Since, the technique has been routinely applied in the design of CO₂ space missions (*Patra et al.*, 2003; *Kadyrov et al.*, 2009; *Kaminski et al.*, 2010; *Rayner et al.*, 2014) and the extension of the in situ sampling network for atmospheric carbon dioxide. Recent examples focus on in situ networks over Australia (*Ziehn et al.*, 2014) and South Africa (*Nickless et al.*, 2014). The design of a combined atmospheric and terrestrial network of the European carbon cycle is addressed by *Kaminski et al.* (2012).

The present study applies the QND concept to the Arctic sea ice-ocean system. It describes the Arctic Observational Network Design (AOND) system, a tool that can evaluate the performance of observational networks comprising a range of different data streams. We illustrate the utility of the tool by evaluating the relative merits of alternate airborne transects within the context of NASA's Operation IceBridge (*Richter-Menge and Farrell*, 2013; *Kurtz et al.*, 2013a), assessing their potential to improve ice forecasts in the Chukchi Sea and along the Alaskan coast.

2 Methods

Our AOND system evaluates observational networks in terms of their impact on target quantities in a data assimilation system. Both the data assimilation system and the AOND system are built
60 around the same model of the Arctic ocean sea-ice system. Below, we first present the model, then the assimilation system and finally the QND approach operates on top of this model.

2.1 NAOSIM

The model used for the present analysis is the coupled ice-ocean model NAOSIM (North Atlantic/Arctic Ocean Sea Ice Model, *Kauker et al.* (2003)). NAOSIM is based on version 2 of the
65 Modular Ocean Model (MOM-2) of the Geophysical Fluid Dynamics Laboratory (GFDL). The version of NAOSIM used here has a horizontal grid spacing of 0.5° on a rotated spherical grid. The rotation maps the $30^\circ W$ meridian onto the equator and the North Pole onto $0^\circ E$. Hence, the model's x- and y-directions are different from the zonal and meridional directions. In the vertical it is resolved by 20 levels, their spacing increasing with depth. The ocean model is coupled to a sea-ice model
70 with viscous-plastic rheology. At the open boundary near $50^\circ N$ the barotropic transport is prescribed from a coarser resolution version of the model that covers the whole Atlantic northward of $20^\circ S$ (*Koeberle and Gerdes*, 2003). Atmospheric forcing (10m-wind velocity, 2m-air temperature, 2m-dew point temperature, total precipitation, and total cloud cover) is taken from the National Centers for Environmental Prediction/National Centre for Atmospheric Research (NCEP/NCAR) reanalysis
75 (*Kalnay and Coauthors*, 1996). This study is based on a model integration from 1 April 2007 to 31 August 2007. The initial state of this integration is the final state of a hindcast from January 1948 to end of March 2007, forced by NCEP/NCAR reanalyses and in turn initialized from PHC (*Steele et al.*, 2001) (ocean temperature and salinity) and a constant ice thickness of 2m with 100% ice cover where the air temperature is below the freezing temperature of the ocean's top layer. The model's
80 process formulations depend on a number of uncertain parameters. Table 1 summarises atmospheric forcing fields, initial fields and lists a subset of the model's relevant process parameters.

2.2 Assimilation

The variational assimilation system NAOSIMDAS (*Kauker et al.*, 2009, 2010) operates through minimisation of a cost function that quantifies the fit to all observations plus the deviation from prior
85 knowledge on a vector of control variables x :

$$J(\tilde{\mathbf{x}}) = \frac{1}{2} [(M(\tilde{\mathbf{x}}) - \mathbf{d})^T \mathbf{C}(d)^{-1} (M(\tilde{\mathbf{x}}) - \mathbf{d}) + (\tilde{\mathbf{x}} - \mathbf{x}_0)^T \mathbf{C}(x_0)^{-1} (\tilde{\mathbf{x}} - \mathbf{x}_0)] \quad (1)$$

where M denotes the model, considered as a mapping from the control vector to observations, d the observations with data uncertainty covariance matrix $\mathbf{C}(d)$, x_0 the vector of prior values of the control variables with uncertainty covariance matrix $\mathbf{C}(x_0)$, and the superscript T is the transposed.

90 The control variables are typically a combination of the initial state, the atmospheric forcing and the

process parameters. The data uncertainty $\mathbf{C}(d)$ reflects the combined effect of observational $\mathbf{C}(d_{\text{obs}})$ and model error $\mathbf{C}(d_{\text{mod}})$:

$$\mathbf{C}(d)^2 = \mathbf{C}(d_{\text{obs}})^2 + \mathbf{C}(d_{\text{mod}})^2 \quad (2)$$

$\mathbf{C}(d_{\text{mod}})$ captures all uncertainty in the simulation of the observations except for the uncertainty in
 95 the control vector, because this fraction of the uncertainty is explicitly addressed by the assimilation
 procedure through correction of the control vector.

2.3 QND

We provide a brief description of the methodological background for QND, which follows *Kaminski
 and Rayner* (2008). The approach is based on propagation of uncertainty from the data to a target
 100 quantity of interest. The target quantity can be any aspect that is extractable from a simulation with
 the underlying model, for example, the sea-ice concentration integrated over a particular domain and
 time period.

QND proceeds in two steps. In the first step, the second derivative (Hessian) of the cost function
 (equation (1)) is used to approximate the inverse of the covariance matrix $\mathbf{C}(x)$ of posterior uncer-
 105 tainty of the control vector, which quantifies the uncertainty ranges of the control variables that are
 consistent with uncertainties in the observations and the model. Denoting the linearisation of the
 model by \mathbf{M}' we can approximate this posterior uncertainty by

$$\mathbf{C}(x)^{-1} = \mathbf{M}'^T \mathbf{C}(d)^{-1} \mathbf{M}' + \mathbf{C}(x_0)^{-1}. \quad (3)$$

In the second step, the linearisation \mathbf{N}' (Jacobian) of the model N used as a mapping from the
 110 control vector to target quantities is employed to propagate the uncertainties in the control vector
 forward to the uncertainty in a target quantity $\sigma(y)$:

$$\sigma(y)^2 = \mathbf{N}' \mathbf{C}(x) \mathbf{N}'^T + \sigma(y_{\text{mod}})^2. \quad (4)$$

If the model was perfect, $\sigma(y_{\text{mod}})$ would be zero. In contrast, if the control variables were perfectly
 known, the first term on the right hand side would be zero.

115 We note that (through equation (3) and equation (4)) the posterior target uncertainty solely depends
 on the prior and data uncertainties as well as the linearised model responses of simulated observation
 counterparts and of target quantities. The approach does not require real observations, and can thus
 be employed to evaluate hypothetical candidate networks. Candidate networks are defined by a set
 of observations characterised by observational data type, location, time, and data uncertainty. Hence,
 120 the QND approach does not require running the assimilation system. By a network we understand
 the complete set of observations, d , used to constrain the model. The term network is not meant to
 imply that the observations are of the same type or that their sampling is coordinated. For example,
 a network can combine in situ and satellite observations.

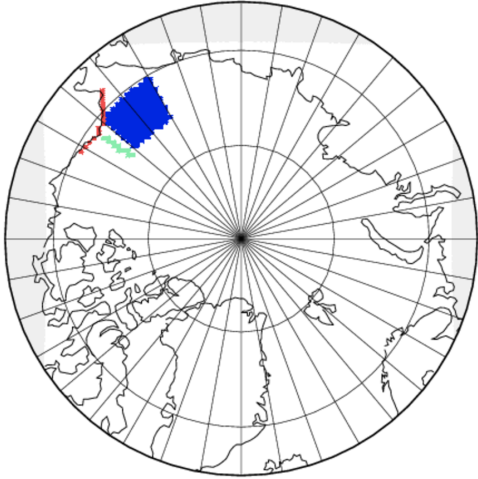


Fig. 1. Target Regions: *Chukchi (blue); North of Barrow (NOB, green) Bering Strait to Prudhoe Bay (BS2PB, red).*

In practice, for pre-defined target quantities and observations, model responses can be pre-
 125 computed and stored. A network composed of these pre-defined observations, can then be evaluated
 in terms of the pre-defined target quantities without further model evaluation. Only matrix algebra
 is required to combine the pre-computed sensitivities with the data uncertainties. This aspect is ex-
 ploited in our AOND system The linearised response functions were computed by the tangent linear
 version of NAOSIM generated from the model's source code through the automatic differentiation
 130 tool TAF (*Giering and Kaminski, 1998*).

3 Experimental setup

3.1 Target Quantities

The goal of this study is to explore the utility of the AOND system in guiding observations for
 short-term to seasonal-scale sea-ice predictions. Ice forecasting at these time scales has been identi-
 135 fied as a high priority in the context of safe maritime operations (*Richter-Menge, 2012; Kurtz et al.,*
2013a; Eicken, 2013) management of marine living resources (*Robards et al., 2013*) and food secu-
 rity for indigenous communities (*Brubaker et al., 2011*). Here, we focus on the first two issues in
 the Chukchi and Beaufort Seas north of Alaska (figure 1 and figure 2), which are experiencing some
 of the highest reductions in summer ice concentration anywhere in the Arctic, along with major
 140 offshore hydrocarbon exploration and potential impacts on protected species such as walrus (*Eicken*
and Mahoney, 2014). Thus, the selection of target quantities for the AOND system seeks to evaluate
 and improve predictions aimed at the information needs of stakeholders and resource managers for

this region.

For all regions delineated in figure 1, we use spatial averages of ice concentration (fraction of area covered by ice, regardless of the 15% floor used in the definition of ice extent), ice thickness, and snow thickness. For each of the target regions we look at these quantities on different days or time periods. For the target region Chukchi we use the above three quantities for each of April 10, June 30, and August 31, yielding a total of nine target quantities. In order to specifically address information needs with respect to safe shipping between Bering Strait and central and eastern Beaufort Sea (including supply of coastal communities and the oil industry hub at Prudhoe Bay, offshore resource exploration and transits through the Northwest Passage), we evaluate an additional set of target quantities derived from the Barnett Ice Severity Index (BSI). The BSI has developed into a standard measure of shipping conditions and potential hazards encountered along the Alaskan coast and at a critical chokepoint of the Northwest Passage and is routinely issued by ice services (*Barnett, 1976*). (*Drobot, 2003*) has examined the predictive skill of statistical models in BSI seasonal forecasts. The BSI is a composite of eight aspects of summer ice conditions (see Table 2), four related to the distance of the ice pack north of Point Barrow (NOB) in mid-August and mid-September and four related to the timing of ice retreat along the sea route from Bering Strait to Prudhoe Bay during the entire navigation season (BS2PB). In replicating these variables in condensed way, we identify the two target regions as shown in figure 1. The target region NOB covers a corridor of 50 km (one grid cell) width extending from Point Barrow to 70° N on August 10 and 31. We use August 31 in contrast to September 15 (which is used in the definition of the BSI), because from end of August to mid September 2007 the ice edge moved northwards of 70° N. For the region BS2PB, in keeping with the BSI we use the time period from May to August.

3.2 Control Variables

In our variational assimilation system the largest possible control vector is the superset of initial and surface boundary conditions as well as all parameters in the process formulations. To keep our AOND system numerically efficient, two- and treedimensional fields are grouped into regions. We proceeded by dividing the Arctic domain into nine regions (figure 2). In each of these regions we add a scalar perturbation to each of the forcing fields (indicated in Table 1 by the type *boundary*). Likewise we add a scalar perturbation to five initial fields (indicated in Table 1 by the type *initial*). For the ocean temperature and salinity the size of the perturbation is reduced with increasing depth. Finally we have selected 18 process parameters from the sea ice-ocean model. This procedure resulted in a total of 128 control variables, a superset of the set of control variables identified by (*Sumata et al., 2013*) to have largest impact on the simulation. Unlike the study by *Kauker et al. (2009)* the control vector used here also includes process parameters. We conducted sensitivity experiments in which we remove components from the control vector. For example, removing the atmospheric forcing explores the (hypothetical) case of a perfect seasonal atmospheric forecast and removing the process

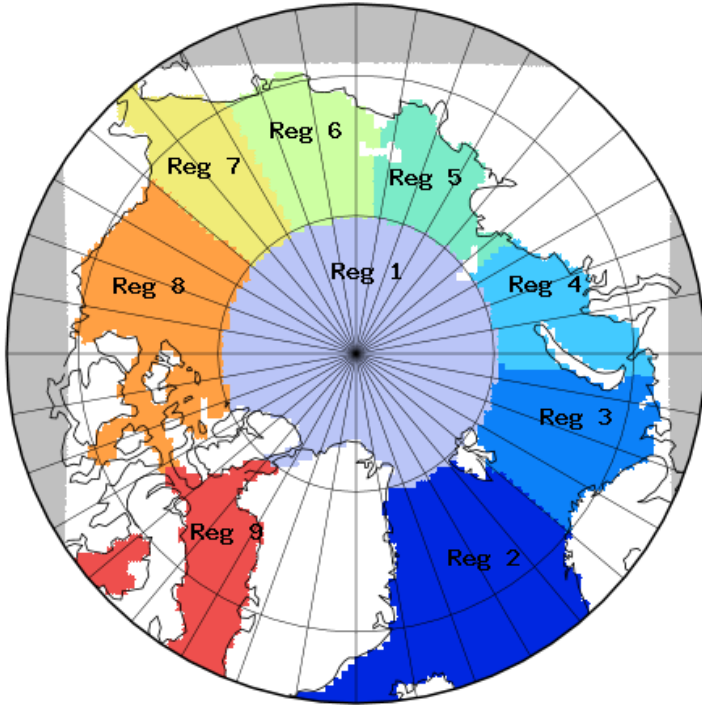


Fig. 2. Regions used in the study. 1 (light plum) central Arctic. 2 (dark blue) North Atlantic, and then counterclockwise to 7 (yellow) Bering Strait/Chukchi Sea, 8 (orange) Beaufort Sea, 9 (red).

parameters the (hypothetical) case of a perfectly calibrated model.

180 The prior uncertainty of the control variables, $C(x_0)$ (see equation (1) and equation (3)) is, assumed to have diagonal form, i.e. there are no correlations among the prior uncertainty relating to different components of the control vector. The diagonal entries are the square of the prior standard deviation. For process parameters this standard deviation is estimated from the range of values typically used within the modelling community. The standard deviation for the components of the initial state, is based on a model simulation over the past twenty years and computed for the twenty member ensemble corresponding to all states on the same day of the year. Likewise the standard deviation for the surface boundary conditions is computed for the twenty member ensemble corresponding to all five-month forecast periods starting on the same day of the year.

3.3 Observational Networks

190 There are various types of observations sampling the Arctic ocean sea-ice system, many of which are potentially suitable for assimilation into a model like NAOSIMDAS. Our AOND system focuses on observations of ice concentration, snow and ice thickness. It provides response functions for each of these three observables, for each surface grid cell, and for each day of the simulation period (i.e. about 5 million possible observations) with a user-defined data uncertainty. In this study we

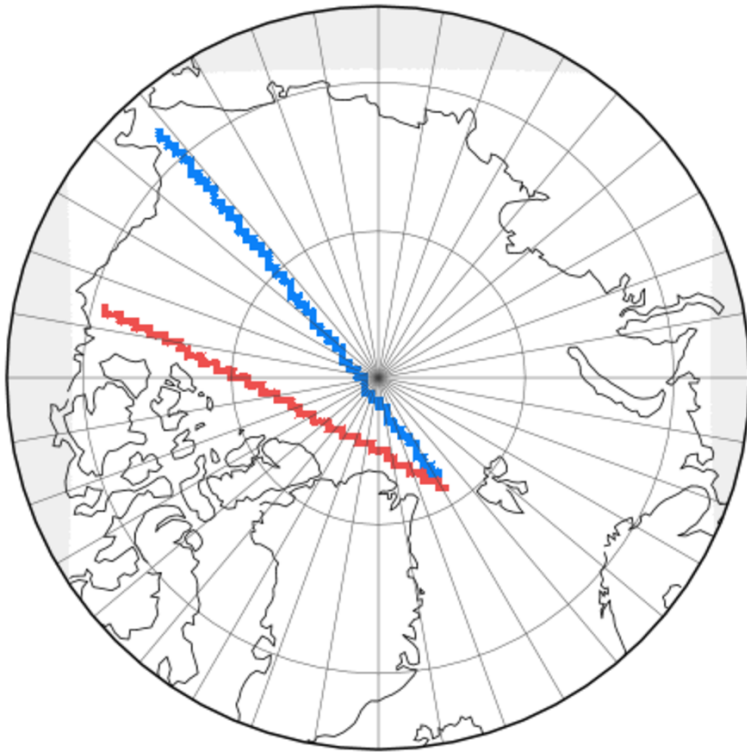


Fig. 3. Flight transects: Chukchi to Fram (C2F, blue); Beaufort to Fram (B2F, red)

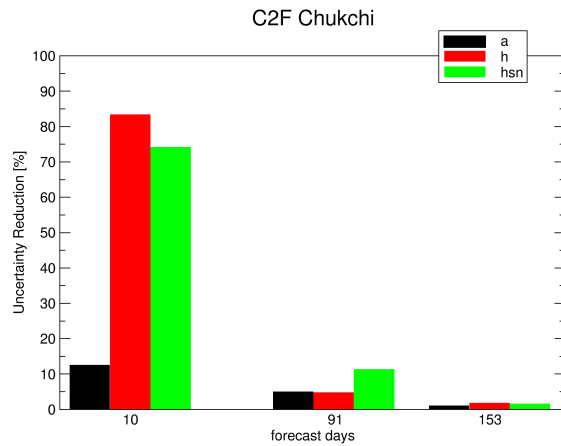
195 demonstrate the application and potential utility of the system in evaluating the relative merits and quantitative contribution to improving sea-ice forecasts for two alternate ice-thickness airborne survey profiles. This example is based on the need for objective guidance on flight routing as part of NASA's Operation IceBridge, an airborne laser altimeter and snow radar campaign meant to provide information on the mass budget of the Arctic ice pack (*Richter-Menge and Farrell, 2013*). Recent

200 work has demonstrated the utility of such data, collected in spring for initialization and constraints on seasonal forecasts of summer ice extent (*Lindsay et al., 2012; Kurtz et al., 2013a*). Based on an evaluation of flown and hypothetical IceBridge transects, we evaluate the impact of simulated measurements along two transects within AOND. The first is a transect from Bering Strait to Fram Strait, which we denote by Chukchi to Fram (C2F, figure 3, blue colour) and the second from Beaufort Sea

205 to Fram Strait which we denote by Beaufort to Fram (B2F, figure 3, red colour). Both flights are assumed to take place on April 5, 2007. The observations consist of model output of ice and snow thickness at each grid cell that intersects with the transect as indicated in figure 3. The default case specifies a data uncertainty of 30 cm for both quantities. To explore the sensitivity of the results with respect to the data uncertainty, we also test a data uncertainty of 10 cm. While the former is

210 at the lower end of what is expected for IceBridge altimeter data (*Kurtz et al., 2013b*), the latter

Panel a



Panel b

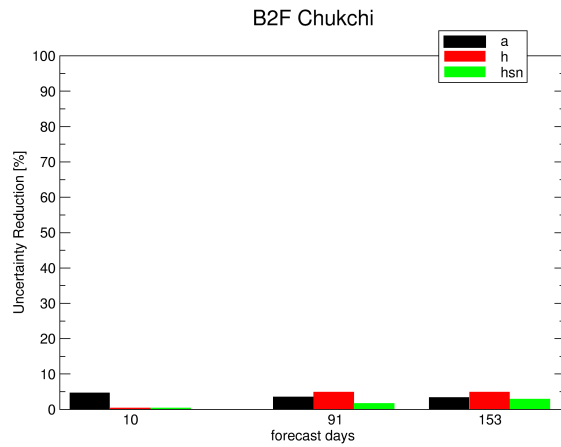


Fig. 4. Uncertainty reduction for the Chukchi target area for flight transect C2F (panel a) and B2F (panel b).

corresponds to the lower bounds of airborne electromagnetic induction measurements (*Haas et al., 2009*).

4 Results and discussion

Figure 4 shows the performance of each transect in improving forecasts over the Chukchi target region. We define the uncertainty reduction relative to the case without observational constraints, where the prior uncertainty in the control vector (see section 3.2) is propagated to the three target quantities. Overall we note a larger impact of C2F on the short-term forecast (10 days) while for B2F the impact increases for the mid-term forecast (3 months). C2F surpasses B2F with respect to the impact on predicted ice concentration and snow thickness, while its impact is marginally smaller

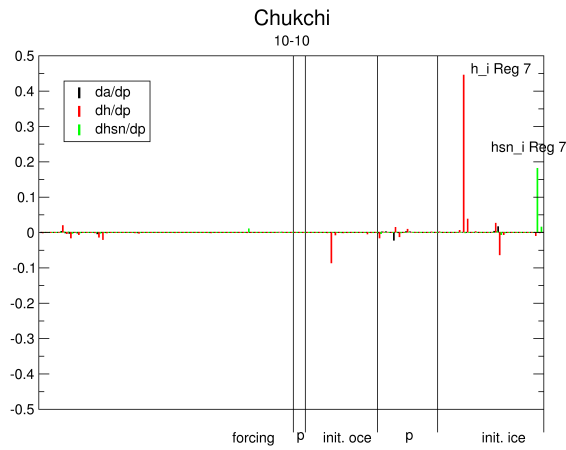
220 for ice thickness. For the 10-day forecast C2F has a much larger impact on predicted ice and snow
thickness than on ice concentration. This is mostly a result of the flights observing specifically the
former two quantities, whereas the model dynamics require some time to transfer any constraints
on snow and ice thickness into constraints on ice concentration. Moreover, ice concentration in
this region is also strongly dependent on factors other than snow and ice thickness, in particular
225 during spring and early summer when the role of wind forcing greatly exceeds that of the other two
variables.

Mathematically, through N' in equation (4), each target quantity defines a one dimensional sub-
space (target direction, *Kaminski et al. (2012)*) of the space spanned by the control vector (control
space). All control vectors v perpendicular to the target direction yield $N'v = 0$. Similarly, through
230 M' in equation (3) each observation defines a second one-dimensional sub-space of the control
space, the observed direction. The better the observed direction projects onto the target direction,
the more efficient is the observation in reducing the uncertainty in the target quantity. According to
equation (3) the uncertainty reduction increases with the response of the observable to a change in
the control vector (M') and decreases with the data uncertainty. Figure 5 provides a visualisation
235 of N' , which shows the response of the three target quantities to a change in each of the control
variables by one standard deviation of prior PDF (table 1). This provides two pieces of information:
First, it shows the target direction, second it shows the size of the impact of an uncertainty reduction
in the target direction. We note that the initial conditions of ice and snow have highest impact for
the short-term forecast. For the mid-term forecast, atmospheric forcing and model parameters also
240 gain in importance. For the interpretation of τ_{ux} and τ_{uy} recall that the model operates on a rotated
coordinate system. Taking the rotation into account, for regions 6, 7, and 8 figure 6 shows the
direction in which a change of τ yields the largest increase in ice thickness. Adding a 25 degrees
Ekman deflection the change of ice motion is towards the target region. For the long-term forecast,
the impacts are generally small, because there is little ice left in the target area.

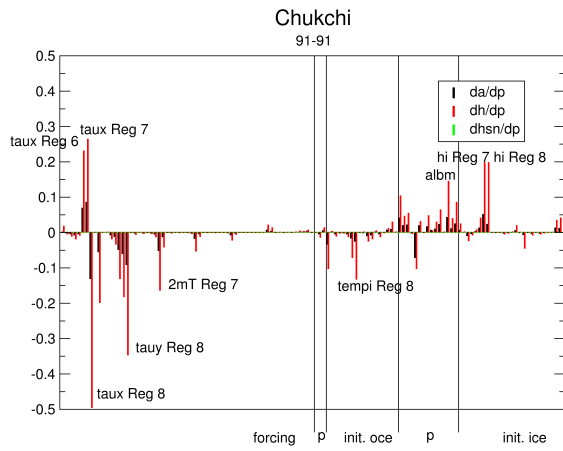
245 Figure 7 shows the performance of each transect for improving forecasts for the target region
covering the coastal ocean from Bering Strait to Prudhoe Bay (BS2PB). They show similar per-
formance with B2F being superior for snow thickness and C2F for ice thickness and area. As an
additional test case we evaluate the combination of the two transects (panel c), which clearly shows
their complementarity.

250 Figure 8 shows the response of the three target quantities to a 1 prior sigma change in each of the
control variables. The impact of wind stress dominates. For both, region 7 and 8, figure 9 shows the
direction in which a change of τ yields the largest increase in ice thickness. Adding a 25 degrees
Ekman deflection the change of ice motion is towards the intersection of the respective region's
coast line with the target area BS2PB. Parameter p_{star} has a positive impact, because it yields more
255 rigid ice. Parameter h_0 has a negative impact: Increasing h_0 yields thicker newly formed ice and
consequently reduces the ice concentration.

Panel a



Panel b



Panel c

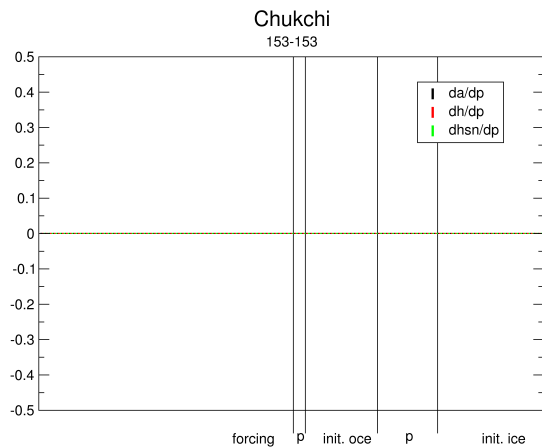


Fig. 5. Sensitivity of target quantities over Chukchi area for 10 day (panel a), 91 day (panel b) and 153 day (panel c) forecasts to 1 sigma prior uncertainty change in each control variable. Units of target quantities (and their sensitivities): ice concentration (a) (0-1); ice thickness (h) in m; snow thickness (hsn) in m.

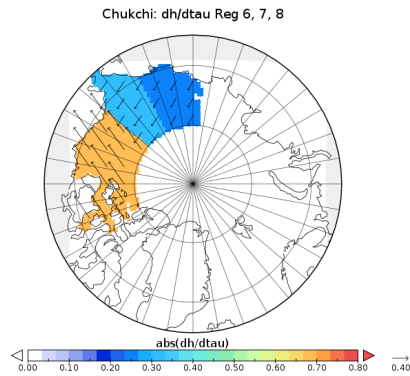


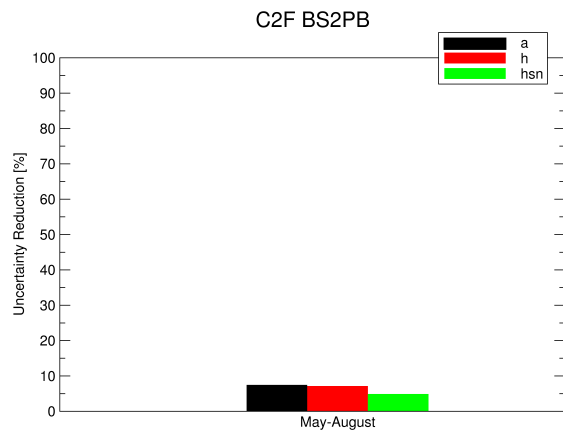
Fig. 6. Wind stress direction with highest impact of tau component in control vector on ice thickness in Chukchi target region. Colour indicates magnitude.

Figure 10 shows the performance of each transect for improving forecasts over the NOB target region. The performance of B2F is much better than that of C2F for both forecast times. This result appears counter-intuitive, because C2F is much closer than B2F, but can be explained through the influence of the westward circulation prevailing in the waters off the Alaskan coast (*Eicken and Mahoney, 2014*). For forecast times of 4-5 months, an upstream observation is associated with much more predictive skill than an observation directly over the target area. In fact the same mechanism explains the previously mentioned higher uncertainty reduction of B2F for the long-term forecast in the Chukchi area. For the target area BS2PB none of the transects dominate, because the target period is an integral from forecast months 2 to 5.

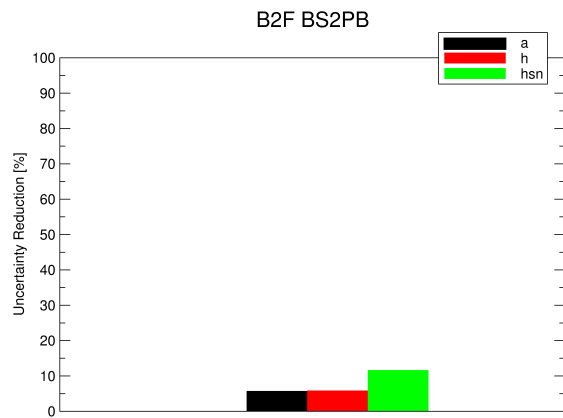
Figure 11 shows the response of the three target quantities (on both, August 10 and 31) to a 1 prior sigma change in each of the control variables. We note the highest impact for tau in region 8 (positive impact of southwest increase) leading to more ice in the target region (see figure 12). Furthermore there is relatively high impact of other atmospheric forcing variables, but also of some parameters (the albedo of melting ice, *albm*, and the ice strength parameter, *pstar*) and the ice initial conditions. There is generally little difference in the responses for the two forecast periods. This is an indication of the robustness of our linearisation of the coupled ocean sea-ice system and confirms an analysis of *Kauker et al. (2009)* who found, for the same model, moderate difference between the linearisation and finite size perturbations.

Figure 13 shows the sensitivity of the performance of (the superior) B2F transect with respect to various impact factors. The reduction in data uncertainty from 0.3 m to 0.1 m for both ice and snow thickness yields a considerable improvement in performance (panel a). The effect is particularly pronounced for ice area. Reducing the prior uncertainty for the atmospheric forcing to zero mimics the availability of a perfect seasonal atmospheric forecast. Under this assumption, the performance of the B2F transect is strongly increased (panel b). Likewise a reduction of the prior uncertainty for all process parameters mimics a perfectly calibrated model. Its effect on the performance of the B2F

Panel a



Panel b



Panel c

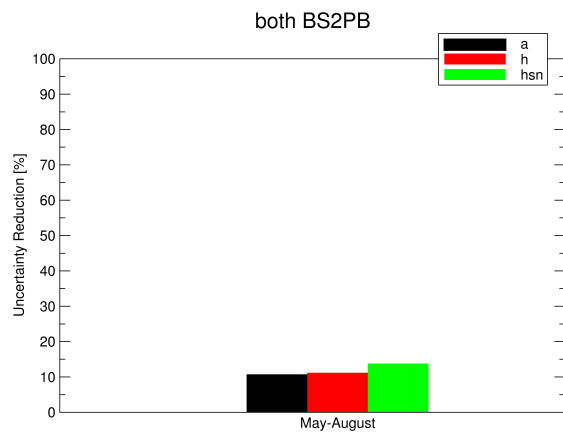


Fig. 7. Uncertainty reduction for target area BS2PB for flight transect C2F (panel a) and B2F (panel b) and both (panel c).

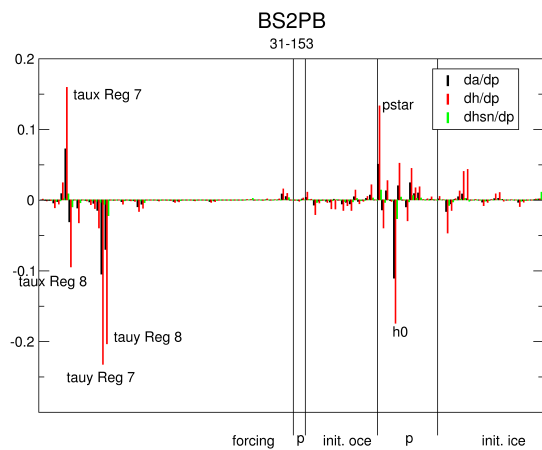


Fig. 8. Sensitivity of target quantities for BS2PB area to 1 sigma prior uncertainty change in each control variable. Units of target quantities (and their sensitivities): ice concentration (a) (0-1); ice thickness (h) in m; snow thickness (hsn) in m.

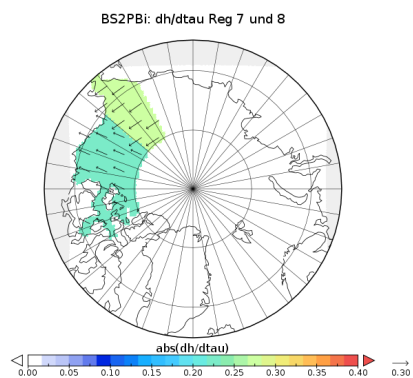
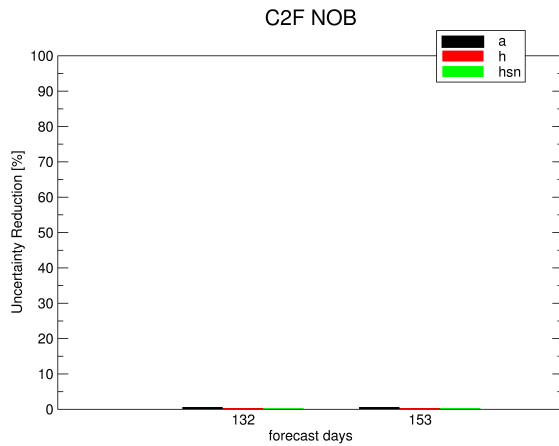


Fig. 9. Wind stress direction with highest impact of tau component in control vector on ice thickness in BS2PB target region. Colour indicates magnitude

Panel a



Panel b

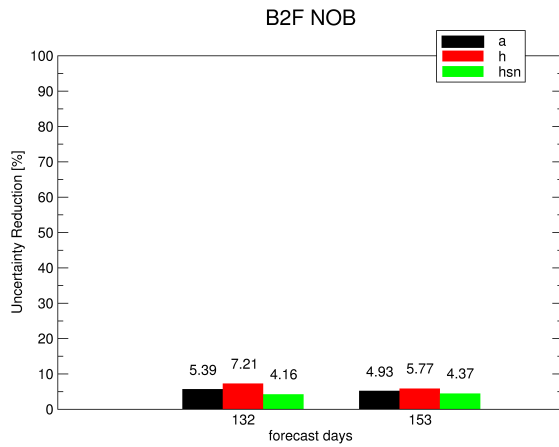


Fig. 10. Uncertainty reduction for target areas NOB for flight transect C2F (panel a) and B2F (panel b).

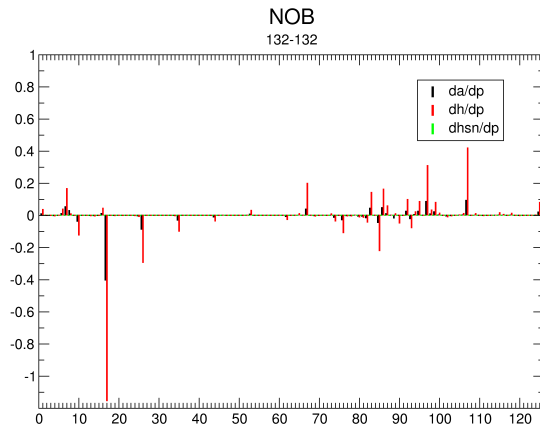
transect is relatively small (panel c). Interestingly, combining the perfectly calibrated model and the perfect atmospheric forecast assumptions doubles the uncertainty reductions compared to the perfect atmospheric forecast assumptions alone.

285 5 Conclusions

We presented an Arctic Observational Network Design (AOND) System that evaluates hypothetical observational networks of the coupled ocean sea-ice system in terms of their constraint of target quantities of interest within an assimilation system.

We apply the tool to evaluate the potential of two flight transects to reduce uncertainties in ice
290 forecasts over periods from ten days to five-months for regions with high offshore (Chukchi Sea)

Panel a



Panel b

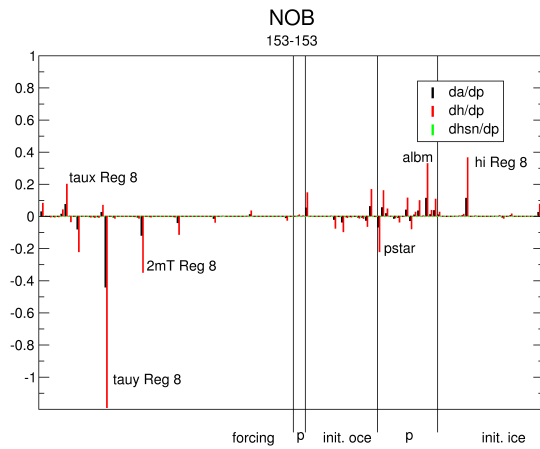


Fig. 11. Sensitivity of target quantity over NOB area for 132 day (panel a), and 153 day (panel b) forecasts to 1 sigma prior uncertainty change in each control variable. Units of target quantities (and their sensitivities): ice concentration (a) (0-1); ice thickness (h) in m; snow thickness (hsn) in m.

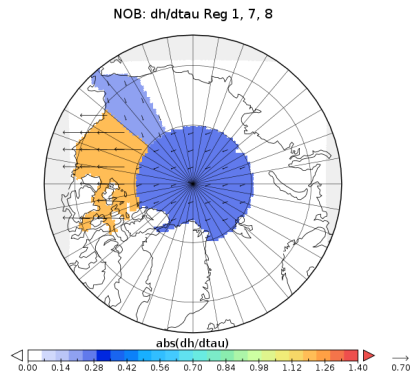


Fig. 12. Wind stress direction with highest impact of tau component in control vector on ice thickness in NOB target region. Colour indicates magnitude

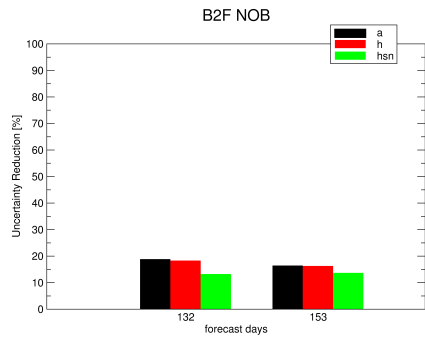
or shipping activity (North-West Passage). For our analysis we deliberately selected the year 2007, a year of particularly low ice extent, which one may regard as representative in terms of future ice conditions under climate change. Clearly, our quantitative results are specific to the conditions in this year. The present study has thus the character of a demonstration, and we focus here on general lessons. Our most general finding is that the network performance depends on the question we ask, i.e. on the target quantity. Next, the longer the forecast time, the further upstream we have to sample, rather than sampling over the target area. Further, we demonstrated in a quantitative way how the model dynamics transfer the observational information on one set of variables (snow and ice thickness) to another variable (ice area).

When defining candidate networks to be evaluated it is essential to take logistic constraints into account. Also, an essential input to the tool is the data uncertainty, which is the combination of uncertainties in the observation and in modelling its counterpart (model uncertainty). These two requirements make clear that a QND tool can only be reasonably operated by a team consisting of observationalists and modellers.

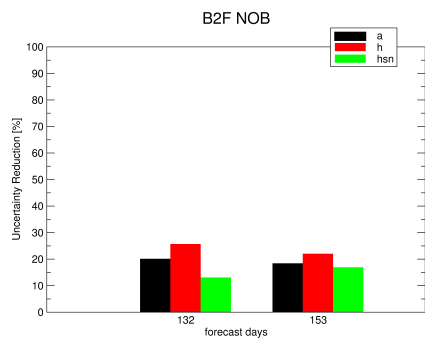
We note that the above-mentioned model uncertainty to be provided to the tool does not necessarily need to refer to the model we use. As long as the response functions of our model are approximately correct, we can use the present system to simulate the observational impact on a assimilation system around a different model. For QND results to be valid beyond the model at hand, one has to used a well-validated model, which includes all relevant processes.

The current AOND system has the flexibility to also evaluate the potential of space missions or further in situ sampling strategies. There are a number of obvious ways to refine the present system. It can be extended to cover climate conditions of further years, possibly also representative of the state of the Arctic as expected under climate change. Also, one could add oceanic observations, further target quantities, or extend the control vector. Furthermore, rather than operating Arctic-

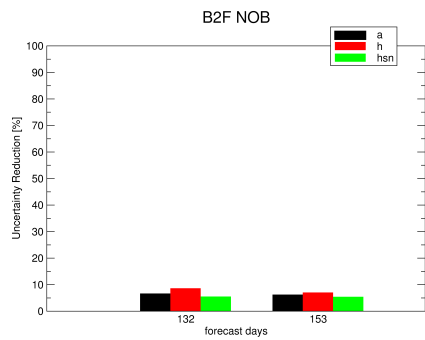
Panel a



Panel b



Panel c



Panel d

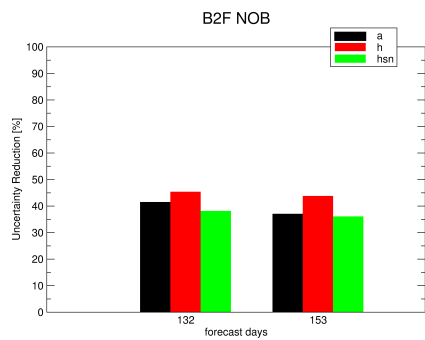


Fig. 13. Uncertainty reduction for target areas NOB for flight transect B2F with data uncertainty of 0.1 m (panel a), the assumption of perfectly known atmospheric forcing (panel b), the assumption of a perfectly calibrated model (panel c), the assumption of perfectly known atmospheric forcing and of a perfectly calibrated model (panel d),

315 wide, the same concept can be applied on smaller regional scale.

Acknowledgements. This work is funded by the European Commission through its Seventh Framework Programme Research and Technological Development under contract number 265863 (ACCESS).

References

- Barnett, D. G., A practical method of long-range ice forecasting for the north coast of alaska, part i, *Technical Report TR-I. Suitland, Maryland: Fleet Weather Facility*, 1976.
- 320 Brubaker, M., J. Berner, R. Chavan, and J. Warren, Climate change and health effects in northwest alaska, *Glob. Health Action*, 4, 2011.
- Crisp, D., et al., The orbiting carbon observatory (oco) mission. trace constituents in the troposphere and lower stratosphere, *Advances in Space Research*, 34, 700 – 709, 2004.
- 325 Drobot, S., Long-range statistical forecasting of ice severity in the beaufort-chukchi sea, *Weather and Forecasting*, 18, 1161–1176, 2003.
- Eicken, H., Arctic sea ice needs better forecasts, *Nature*, 497, 431–433, 2013.
- Eicken, H., and A. R. Mahoney, Sea ice: Hazards, risks and implications for disasters, in *Ellis, J., Sherman, D. (Eds.), Sea and ocean hazards*, Elsevier, Oxford, 2014.
- 330 Giering, R., and T. Kaminski, Recipes for Adjoint Code Construction, *ACM Trans. Math. Software*, 24, 437–474, 1998.
- Haas, C., J. Lobach, S. Hendricks, L. Rabenstein, and A. Pfaffling, Helicopter-borne measurements of sea ice thickness, using a small and lightweight, digital em system, *J. Appl. Geophys.*, 67, 234–241, 2009.
- Hardt, M., and F. Scherbaum, The design of optimum networks for aftershock recordings, *Geophys. J. Int.*, 117, 335 716–726, 1994.
- Kadygrov, N., S. Maksyutov, N. Eguchi, T. Aoki, T. Nakazawa, T. Yokota, and G. Inoue, Role of simulated gosat total column co2 observations in surface co2 flux uncertainty reduction, *Journal of Geophysical Research: Atmospheres*, 114, n/a–n/a, 2009.
- Kalnay, E., and Coauthors, The ncep/ncar 40-year reanalysis project, *Bull. Amer. Meteor. Soc.*, 77, –33, 1996.
- 340 Kaminski, T., and P. J. Rayner, Assimilation and network design, in *Observing the continental scale Greenhouse Gas Balance of Europe*, edited by H. Dolman, A. Freibauer, and R. Valentini, Ecological Studies, chap. 3, Springer-Verlag, New York, 2008.
- Kaminski, T., M. Scholze, and S. Houweling, Quantifying the Benefit of A-SCOPE Data for Reducing Uncertainties in Terrestrial Carbon Fluxes in CCDAS, *Tellus B*, 62, 784–796, 2010.
- 345 Kaminski, T., P. J. Rayner, M. Voßbeck, M. Scholze, and E. Koffi, Observing the continental-scale carbon balance: assessment of sampling complementarity and redundancy in a terrestrial assimilation system by means of quantitative network design, *Atmospheric Chemistry and Physics*, 12, 7867–7879, 2012.
- Kauker, F., R. Gerdes, M. Karcher, C. Köberle, and J. Lieser, Variability of Arctic and North Atlantic sea ice: A combined analysis of model results and observations from 1978 to 2001, *Journal of Geophysical Research Oceans*, 108, 13–1, 2003.
- 350 Kauker, F., T. Kaminski, M. Karcher, R. Giering, R. Gerdes, and M. Voßbeck, Adjoint analysis of the 2007 all time arctic sea-ice minimum, *Geophysical Research Letters*, 2009.
- Kauker, F., R. Gerdes, M. Karcher, T. Kaminski, R. Giering, and M. Voßbeck, June 2010 Sea Ice Outlook - AWI/FastOpt/OASys, Sea Ice Outlook web page, 2010.
- 355 Koeberle, C., and R. Gerdes, Mechanisms determining the variability 2003: Mechanisms determining the variability of Arctic sea ice conditions and export, *J. Clim.*, 16, 2843–2858, 2003.
- Kurtz, N. T., J. Richter-Menge, S. Farrell, M. Studinger, J. Paden, J. Sonntag, and J. Yungel, Icebridge airborne

- survey data support arctic sea ice predictions, *EOS, Transactions American Geophysical Union*, 94, 2013a.
- 360 Kurtz, N. T., S. L. Farrell, M. Studinger, N. Galin, J. P. Harbeck, R. Lindsay, V. D. Onana, B. Panzer, and
J. G. Sonntag, Sea ice thickness, freeboard, and snow depth products from operation icebridge airborne data,
Cryosphere, 7, 1035–1056, 2013b.
- Lindsay, R., et al., Seasonal forecasts of arctic sea ice initialized with observations of ice thickness, *Geophys.
Res. Lett.*, 39, L21,502, 2012.
- 365 Nickless, A., T. Ziehn, P. J. Rayner, R. J. Scholes, and F. Engelbrecht, Greenhouse gas network design using
backward lagrangian particle dispersion modelling; part 2: Sensitivity analyses and south african test case,
Atmospheric Chemistry and Physics Discussions, 14, 11,301–11,342, 2014.
- O'Brien, D. M., and P. J. Rayner, Global observations of the carbon budget, 2, co2 column from differential
absorption of reflected sunlight in the 1.61 m band of co2, *Journal of Geophysical Research: Atmospheres*,
107, ACH 6–1–ACH 6–16, 2002.
- 370 Patra, P. K., S. Maksyutov, Y. Sasano, H. Nakajima, G. Inoue, and T. Nakazawa, An evaluation of co2 obser-
vations with solar occultation fts for inclined-orbit satellite sensor for surface source inversion, *Journal of
Geophysical Research: Atmospheres*, 108, n/a–n/a, 2003.
- Rayner, P. J., and D. M. O'Brien, The utility of remotely sensed CO₂ concentration data in surface source
inversions, *Geophys. Res. Lett.*, 28, 175–178, 2001.
- 375 Rayner, P. J., I. G. Enting, and C. M. Trudinger, Optimizing the CO₂ observing network for constraining sources
and sinks, *Tellus*, 48B, 433–444, 1996.
- Rayner, P. J., R. M. Law, D. M. O'Brien, T. M. Butler, and A. C. Dilley, Global observations of the carbon
budget 3. initial assessment of the impact of satellite orbit, scan geometry, and cloud on measuring co2 from
space, *Journal of Geophysical Research: Atmospheres*, 107, ACH 2–1–ACH 2–7, 2002.
- 380 Rayner, P. J., S. R. Utembe, and S. Crowell, Constraining regional greenhouse gas emissions using geostation-
ary concentration measurements: a theoretical study, *Atmospheric Measurement Techniques Discussions*, 7,
1367–1392, 2014.
- Richter-Menge, J. A., Seasonal-to-decadal predictions of arctic sea ice: Challenges and strategies, in *Committee
on the Future of Arctic Sea Ice Research in Support of Seasonal to Decadal Predictions*, National Academies
385 Press, Washington, DC, 2012.
- Richter-Menge, J. A., and S. L. Farrell, Arctic sea ice conditions in spring 2009-2013 prior to melt, 40, 2013.
- Robards, M., J. Burns, C. Meek, and A. Watson, Limitations of an optimum sustainable population or poten-
tial biological removal approach for conserving marine mammals: Pacific walrus case study, *J. Environm.
Managem.*, 91, 57–66, 2013.
- 390 Steele, M., R. Morley, and W. Ermold, PHC: A global ocean hydrography with a high-quality Arctic Ocean, *J.
Clim.*, 14, 2079–2087, 2001.
- Sumata, H., F. Kauker, R. Gerdes, C. Kberle, and M. Karcher, A comparison between gradient descent and
stochastic approaches for parameter optimization of a sea ice model, *Ocean Sci.*, 9, 609–630, 2013.
- 395 Ziehn, T., A. Nickless, P. J. Rayner, R. M. Law, G. Roff, and P. Fraser, Greenhouse gas network design using
backward lagrangian particle dispersion modelling; part 1: Methodology and australian test case, *Atmo-
spheric Chemistry and Physics Discussions*, 14, 7557–7595, 2014.

Table 1. Control Variables. Column 1 lists the quantities in the control vector, column 2 gives the abbreviation for each quantity, column 3 indicates whether the quantity is an atmospheric boundary (forcing, i.e. f) field, an initial field (i), or a process parameter (p), column 4 gives the name of each quantity, column 5 indicates (the standard deviation of) the prior uncertainty and the corresponding units and provides the magnitude of the parameter value in parenthesis, where applicable, and column 6 identifies the position of the quantity in the control vector; for initial and boundary values (which are differentiated by region) this position refers to the first region, the following components of the control vector then cover regions 2 to 9.

index #	name	type	meaning	prior unc (value)	start
1	taux	f	wind stress model x-component	0.02 Nm^2	1
2	tauy	f	wind stress model y-component	0.02 Nm^2	10
3	2mT	f	2-meter air temperature	1.2 K	19
4	DewT	f	dew point temperature	1.1 K	28
5	cld	f	cloud cover	0.07	37
6	precip	f	total precipitation	$0.4 \times 10^{-8} m/s$	46
7	scalwnd	f	scalar wind speed	0.6 m/s	55
8	kappa _m	p	vertical viscosity coeff.	$0.1 \times 10^{-3} (1.0 \times 10^{-3}) m^2/s$	64
9	kappa _h	p	vertical diffusion coeff.	$1. \times 10^{-5} (1. \times 10^{-5}) m^2/s$	65
10	cdbot	p	bottom drag coeff.	$0.5 \times 10^{-3} (1.2 \times 10^{-3})$	66
11	temp _i	i	initial ocean temperature	0.5 K (vertically decreasing)	67
12	salinity _i	i	initial salinity	0.5 <i>psu</i> (vertically decreasing)	76
13	pstar	p	ice strength	10000 (15000) Nm	85
14	cstar	p	ice strength depend. on ice conc.	5. (20.)	86
15	eccen	p	squared yield curve axis ratio	0.5 (2.)	87
16	gmin	p	regime plastic-linear viscous	$1. \times 10^{-9} (5. \times 10^{-9})$	88
17	h0	p	lead closing	1. (0.5) m	89
18	cdwat	p	ocean drag coeff.	$2. \times 10^{-3} (5.5 \times 10^{-3})$	90
19	cdwin	p	atmosphere drag coeff.	$1. \times 10^{-3} (2.475 \times 10^{-3})$ (absorbed in tau _x /y)	
20	angwat	p	ice turning angle	5.° (25.°)	92
21	cdsens	p	sensible heat flux coeff.	$0.5 \times 10^{-3} (1.75 \times 10^{-3})$	93
22	cdlat	p	latent heat flux coeff.	$0.5 \times 10^{-3} (1.75 \times 10^{-3})$	94
23	albw	p	open water albedo	0.05 (0.1)	95
24	albi	p	freezing ice albedo	0.1 (0.7)	96
25	albm	p	melting ice albedo	0.1 (0.68)	97
26	albsn	p	freezing snow albedo	0.1 (0.8)	98
27	albsnm	p	melting snow albedo	0.1 (0.77)	99
28	h _i	i	initial ice thickness	0.5 m	100
29	a _i	i	initial ice concentration	0.1	109
30	hsn _i	i	initial snow thickness	0.2 m	118

Table 2. Aspects entering the definition of the BSI

Distance from Point Barrow northward to ice edge (10 Aug).

Distance from Point Barrow northward to ice edge (15 Sept).

Distance from Point Barrow northward to boundary of five tenths ice concentration (10 Aug).

Distance from Point Barrow northward to boundary of five tenths ice concentration (15 Sept).

Initial date entire sea route to Prudhoe Bay less than/equal to five tenths ice concentration.

Date that combined ice concentration and thickness dictate end of prudent navigation.

Number of days entire sea route to Prudhoe Bay ice free.

Number of days entire sea route to Prudhoe Bay less than/equal to five tenths ice concentration.
